# Void channel microstructures in resin solids as an efficient way to infrared photonic crystals

M. J. Ventura, M. Straub, and M. Gu[a)]
*Center for Micro-Photonics, School of Biophysical Sciences and Electrical Engineering, Swinburne University of Technology, P.O. Box 218, Hawthorn, Victoria 3122, Australia*

(Received 26 September 2002; accepted 21 January 2003)

Microvoid channels were generated by local melting in a solidified polymer resin sample moving perpendicular to the focus of a high numerical-aperture objective under visible femtosecond-pulsed illumination. Channel size, surface quality, and high density channel vicinity depended on laser intensity and scanning speed. Electron microscope images revealed elliptical channel cross sections of 0.7–1.3 $\mu$m in lateral diameter and an elongation in the focusing direction of approximately 50%. A 20 layer woodpile-type photonic crystal structure with a 1.7 $\mu$m layer spacing and a 1.8 $\mu$m in-plane channel spacing provided a sharp peak in reflection and a suppression of infrared transmission in the stacking direction by 85% at wavelength 4.8 $\mu$m with a gap/midgap ratio of 0.11.
 [DOI: 10.1063/1.1560870]

Fabrication of voids inside transparent bulk materials has found increasing interest in the fields of data storage and microfabrication in recent years. The ability to shape void structures inside a solid material without the requirement to have direct access from the outside promises numerous applications for optical microdevices, micromachines, microsensors, or actuators. Void formation in silica,[1–3] quartz,[1,3] sapphire,[1,3] BK7 optical glass,[1] acrylic plastic,[1] as well as polymethylmethacrylate[4,5] has been investigated. In all these experiments tightly focused ultrashort-pulsed laser light induced microexplosions inside bulk material, leaving voids in their center surrounded by a region of increased density. The main interest in void microstructures so far has concentrated on optical bit-data storage.[1,4,5] Voids are readily generated using high energy amplified laser pulses,[1,4] as their high power can trigger second and even higher order nonlinear damaging processes. Only in polymer material has the damaging threshold been found to be low enough for voids to be generated without a regenerative amplifier.[5] However, the strong structural and refractive-index changes inherent to void formation impair the data readout and limit three-dimensional optical data storage to a small number of layers. By contrast, many applications such as a large variety of photonic crystal structures can be generated based on continuous void structures,[6–8] which are more difficult to achieve than void bits. Such structures can be generated efficiently and with high quality boundaries using low peak power high repetition laser light.

In this letter, we report the generation of continuous-void polymer microstructures and void channel based infrared photonic crystals. We demonstrate that void channel microstructures can be fabricated inside a commercially available precured photopolymer resin, which makes up a transparent bulk solid. High repetition rate, femtosecond pulsed laser light at a wavelength of 540 nm induced microexplosions dispersing material from the focus and leaving voids in its center. Translation of the polymer through the focus resulted in microvoid channels featuring elliptical cross sections perpendicular to the channel axis with smooth, well-defined boundaries. We present a photonic crystal with a high degree of perfection by stacking layers of such void channels in a 20 layer woodpile structure which allows suppression of mid infrared light transmission to as much as 85%.

Figure 1 shows the experimental setup. A 710 nm femtosecond pulsed beam from a 5 W pumped mode-locked Ti:sapphire laser (Mira 900-F; Coherent, Santa Clara, CA) passed through an optical parametric oscillator (Mira-OPO, Coherent; 1065-1265 / 545–625 nm) with an intracavity optical frequency doubler. The resulting beam of wavelength 540 nm had a repetition rate of 76 MHz and a pulse width of 200 fs. A neutral density filter (ND) introduced into the beam path allowed for adjustments in beam intensity. The telescope arrangement led to uniform illumination over the backaperture of an oil immersion objective, Zeiss Plan-Neofluar 40×, with numerical aperture 1.3. During the void channel generation the sample was mounted on a 200

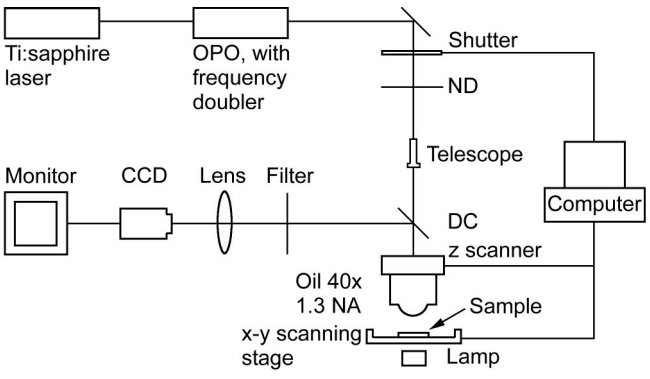


FIG. 1. Optical setup for microfabrication using a high repetition rate, femtosecond-pulsed 540 nm light source. A magnification factor 40, 1.3 NA oil immersion objective focuses the light inside a solidified sample of polymer resin, causing void formation. In-plane translation is controlled by an $x-y$ scanning stage. Moving the objective using a piezoelectric translator controls layer stacking. Fabrication is monitored *in situ* using a CCD camera. OPO, optical parametric oscillator; ND, neutral density filter; DC, dichroic mirror.

a)Electronic mail: mgu@swin.edu.au

 

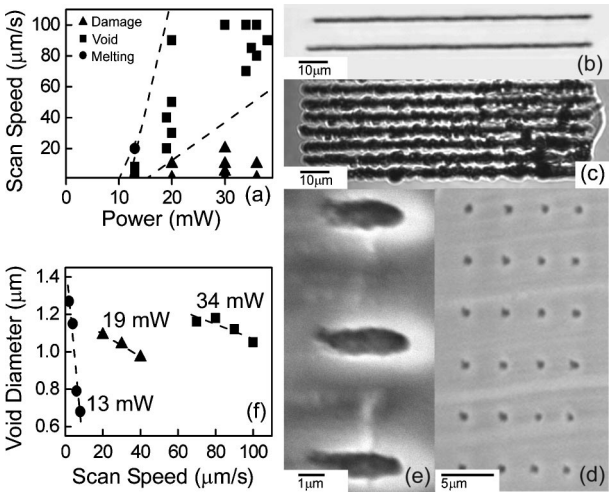


FIG. 2. (a) Material response regions with respect to scan speed and laser intensity. A melting region, a region of void generation, and a damaging region can be distinguished. (b) Light microscope transmission images of smooth and well defined void channels, and (c) void channels in the damaging region fabricated with excess power resulting in rough boundaries and an inhomogeneous shape. (d) Scanning electron microscope images of a periodic arrangement of void channels exiting a cut surface and (e) their elliptical cross section perpendicular to the channel axis. (f) For different intensities and scan speeds the diameters of the void channels can be varied from 1.3 to 0.7 $\mu$m.

$\times 200$ $\mu$m piezoelectric scanning stage (Physik Instrumente, Waldbronn, Germany) for the in-plane motion, whereas the layer spacing was controlled using a 350 $\mu$m piezoelectric translator for the objective (Physik Instrumente). Both the translators and the shutter were computer controlled, and the entire fabrication process was monitored *in situ* by a charge coupled device (CCD) camera gathering the transmission illumination from a halogen lamp beneath the sample as well as fluorescence emission in the focus. The polymerizable material used was Norland NOA 63 resin, which is a polyurethane oligomer having C═C unsaturation and is crosslinked by a mercapto-ester oligomer. The curing process involved exposure of a film of liquid resin sandwiched between glass coverslips to a focused wide band UV light source for a period of 2 h resulting in a transparent, hard polymer with a refractive index of 1.56. The photonic band gap was measured in the infrared transmission and reflection regime in a Fourier-transform infrared microspectroscopy system (Nicolet Nexus/Continuum).

Figure 2 presents the conditions of void channel fabrication as well as their characterization. The response of the polymer varies with respect to laser power and scanning speed. Fig. 2(a) depicts a plot of the four main material response regions. Below a threshold exposure no change in the material was observed. A small region above the threshold allowed the introduction of a change in the refractive index of the material without major structural changes. A further increase of power results in the formation of microvoid channels, as material in the focus is placed under high temperature and pressure leading to microexplosions. The resulting structures [see Fig. 2(b)] are continuous, smooth, and well defined microvoid channels. In the final response region the deposited energy is beyond the limit of smooth channel generation. Microvoid channels can no longer be generated with any consistency. Channel boundaries are rough, as explosion prevents the channels from developing a homogeneous shape and adjacent channels can become merged [see Fig. 2(c)].

Microvoid channels of the smooth channels region were examined in detail using scanning electron microscopy (SEM). Figure 2(d) shows a periodic structure prepared at a power of 20 mW and a scan speed of 95 $\mu$m/s. Both the layer spacing and the in-plane channel spacing amounted to 5 $\mu$m. The structure was sliced through perpendicular to the direction of the void channels using a fine metal blade in order to analyze the channel morphology. The dark points are holes on the surface and show channels exiting from the polymer material. As the SEM image was recorded at a tilt angle of approximately 45° with respect to the channel axis, the layer spacing as well as the channel diameter in the focusing direction appear to be reduced by 30%. Note the high degree of position accuracy in both the focusing and the transverse directions. The cross-sectional dimensions of microvoid channels are of an ellipsoidal shape, elongated in the focusing direction. Figure 2(e) shows the cross sections as recorded almost perpendicular to the axis of three parallel void channels fabricated at a power of 34 mW and a scan speed of 80 $\mu$m/s. The diameters of these channels are 1.9 $\mu$m in the focusing and 1.2 $\mu$m in the transverse direction. The ratio between diameters of 1.6 is much smaller than the corresponding ratio for a multiphoton excitation point spread function, which is for example approximately 3.1 under two-photon excitation for a numerical aperature (NA) 1.3 objective at a wavelength of 540 nm. This is most likely due to the explosion type mechanism of void formation and can be explained by the redistribution of melted material around the focus before its resolidification. In the SEM images the region of higher density around the voids is observed as a bright halo. Its thickness is approximately a few hundred nanometers.

Figure 2(f) plots the transverse channel diameter versus scan speed for three power levels 13, 19, and 34 mW. A linear dependence of cross-sectional dimensionality was observed for a range of powers, which is consistent with the results achieved recently for polymethylmethacrylate.[5] At 13 mW small steps in scan speed result in large swings in microvoid channel diameters, which change from 1.25 to 0.65 $\mu$m over a 6 $\mu$m/s window of speeds. For higher powers channel diameters have a reduced sensitivity to changes in the scan speed. For a writing power of 19 mW channel diameters are varied by 0.3 $\mu$m over a 20 $\mu$m/s range, whereas for 34 mW the same variation of diameter requires twice the scan range of 40 $\mu$m/s. This dependence of the channel diameter on laser intensity and scan speed allows for specific diameters to be generated within the bulk polymer material with a high degree of accuracy.

The possibility to fabricate microvoid channels inside a solid polymer material allows for an efficient generation of polymer photonic crystals. In contrast to microfabrication by photopolymerization of structures in a liquid resin,[9–11] no chemical postprocessing is required to remove unused material. Moreover, there is no need to anchor the structure on any kind of carrier. Commercially available resins can be used, because polymer shrinkage and stability of structural elements do not play a major role inside the solid material. Figure 3 shows a photonic crystal of the woodpile structure

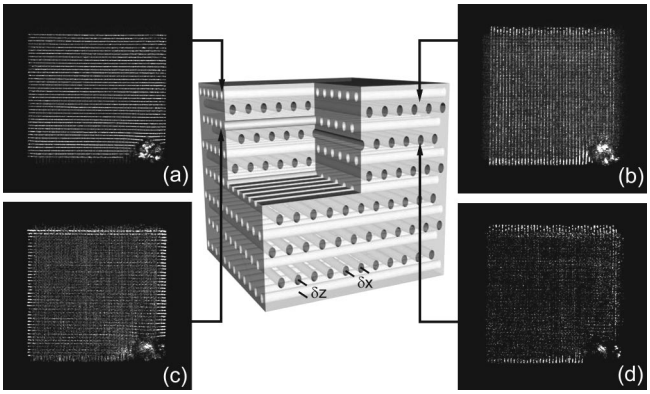


FIG. 3. Sketch of a woodpile structure consisting of elliptical void channels. Alternating layers are stacked perpendicularly with corresponding layers displaced by half an in-plane period. (a)–(d) Reflection confocal microscope images of the top four layers recorded at depths of 0, 1.7, 3.4, and 5.1 $\mu$m.

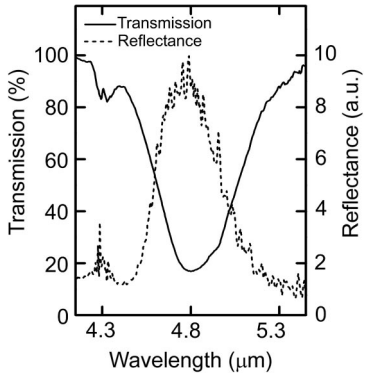


FIG. 4. Infrared transmission and reflection spectra of a 20 layer woodpile structure with $\delta z = 1.7$ $\mu$m layer spacing and $\delta x = 1.8$ $\mu$m in-plane channel spacing. The photonic stop gap in the stacking direction results in suppression of transmission by 85% at a wavelength of 4.75 $\mu$m. In the gap region the infrared reflectance is increased by an order of magnitude.

type as generated by stacking of layers of void channels (35 mW / 120 $\mu$m/s). Woodpile structures allow for sizable photonic band gaps at a large variety of structural parameters.[12,13] Although the low dielectric contrast and the comparatively high filling ratio in our void microstructures prevent band gaps from being complete, large stop gaps exist around the stacking direction. Adjacent layers are perpendicular and corresponding layers are offset by half an in-plane spacing, resulting in a four layer periodicity. By the selection of the in-plane spacing $\delta x$ between parallel channels and the layer spacing $\delta z$ between adjacent channels the photonic stop gap can be tuned to the desired wavelengths. Figures 3(a)–3(d) present reflection confocal images of the first four layers of a $80 \times 80$ $\mu$m 20 layer structure with $\delta x = 1.8$ $\mu$m and $\delta z = 1.7$ $\mu$m at depths of 0, 1.7, 3.4, and 5.1 $\mu$m. The images were acquired by the use of a He–Ne laser beam and a $60\times$ NA 1.25 oil immersion objective. Light scattering by the submicron structural elements prevented us from imaging deeper layers. The photonic stop gap was observed in the infrared transmission and reflection spectra shown in Fig. 4. Suppression of infrared transmission of 85% occurred at a wavelength of 4.75 $\mu$m, and a gap/midgap ratio of 0.11 was determined. The dip in transmission coincided with a sharp peak in the reflectance, which was increased by as much as a factor of 10.

In conclusion, we have generated microvoid channels inside a transparent bulk material of cured photosensitive polymer by translating a sample through the focus of an objective illuminated by a high-repetition rate femtosecond-pulsed beam at wavelength 540 nm. Channels with well defined smooth boundaries can be generated featuring elliptical cross sections elongated in the focusing direction. This method provides an efficient way to fabricate photonic crystals, as demonstrated for a woodpile structure that exhibited a stop gap with high suppression of infrared transmission and strongly increased reflection at a wavelength of 4.75 $\mu$m.

The authors thank the Australian Research Council for its support.

[1] E. N. Glezer, M. Milosavljevic, L. Huang, R. J. Finlay, T.-H. Her, J. P. Callan, and E. Mazur, Opt. Lett. **21**, 2023 (1996).
[2] E. N. Glezer and E. Mazur, Appl. Phys. Lett. **71**, 882 (1997).
[3] W. Watanabe, T. Toma, K. Yamada, J. Nishii, K.-I. Hayashi, and K. Itoh, Opt. Lett. **25**, 1669 (2000).
[4] K. Yamasaki, S. Juodkazis, M. Watanabe, H.-B. Sun, S. Matsuo, and H. Misawa, Appl. Phys. Lett. **76**, 1000 (2000).
[5] D. Day and M. Gu, Appl. Phys. Lett. **80**, 2404 (2002).
[6] E. Yablonovitch, Phys. Rev. Lett. **58**, 2059 (1987).
[7] E. Yablonovitch, T. J. Gmitter, and K. M. Leung, Phys. Rev. Lett. **67**, 2295 (1991).
[8] J. Joannopoulos, R. Meade, and J. Winn, *Photonic Crystals* (Princeton University Press, New York, 1995).
[9] S. Maruo, O. Nakamura, and S. Kawata, Opt. Lett. **22**, 132 (1997).
[10] H.-B. Sun, S. Matsuo, and H. Misawa, Appl. Phys. Lett. **74**, 786 (1999).
[11] M. Straub and M. Gu, Opt. Lett. **27**, 1824 (2002).
[12] S. Ogawa, K. Tomoda, and S. Noda, J. Appl. Phys. **91**, 513 (2002).
[13] D. M. Whittaker, Opt. Lett. **25**, 779 (2000).